condensed matter

MDPI

Communication

Polaronic States and Superconductivity in WO_{3-x}

Ekhard K.H. Salje

Department of Earth Sciences, University of Cambridge, Downing Street, Cambridge CB2 3EQ, UK; Ekhard@esc.cam.ac.uk

Received: 7 April 2020; Accepted: 27 April 2020; Published: 1 May 2020

Abstract: Superconducting domain boundaries were found in WO_{3-x} and doped WO_3. The charge carriers in WO_3-type materials were identified by Schirmer and Salje as bipolarons. Several previous attempts to determine the electronic properties of polarons in WO_3 failed until Bousque et al. (2020) reported a full first principle calculation of free polarons in WO_3. They confirmed the model of Schirmer and Salje that each single polaron is centred around one tungsten position with surplus charges smeared over the adjacent eight tungsten positions. Small additional charges are distributed further apart. Further calculations to clarify the coupling mechanism between polaron to form bipolarons are not yet available. These calculations would help to identify the carrier distribution in Magneli clusters, which were shown recently to contain high carrier concentrations and may indicate totally localized superconductivity in non-percolating clusters.

Keywords: ferroelastic; WO3; polarons; polaronic superconductivity

1. Introduction and Some Historic Background

The discovery of polaronic states in WO_{3-x} is related to Alex Muller. I first met Alex in 1970 during a trip to Zurich to visit my friend Fritz Laves. Fritz was then the most preeminent crystallographer in Europe who was at the heart of rapid developments of diffraction tools and the theory of symmetry and finite groups. I was introduced to him by my mathematics professor Heesch in Hannover, who solved the essentials of the four-colour problem but was then discouraged to publish his work on magnetic space groups by Fritz Laves and Raman because it would serve no good purpose'. A few years later Shubnikov published his famous paper and Heesch took it stoically. I was just starting a PhD and struggled to promote the message that perovskite structures would be a good example of structural instabilities without compromising the macroscopic and chemical integrity of the material. The idea was generally rejected in the solid state community for two opposing reasons: the first argument was that anything beyond Si could not be understood properly because our theoretical framework was insufficient, and, secondly, that the perovskite structure was far too simple to show effects of internal structural instabilities where one would need structures of much greater complexity like garnets, feldspars and boracites.

Fritz Laves had discovered the Laves-phases and I expected to get some support from him for my PhD project. He did so enthusiastically and told me to see Alex Müller in Ruschlikon who knew much about the perovskite structures in ferroelectricity and in particular about $SrTiO_3$. He had published an excellent account of the phonon instability of $LaAlO_3$ [1] and some years later he would publish his famous paper on the quantum paraelectric state of $SrTiO_3$ together with H. Burkhard [2]. I wanted to extend the research of structural phase transitions to include electronic effects and guessed that tungsten would be a good B atom in the perovskite structure for this purpose. A prototypic material that I wanted to research was WO_3 and its derivatives like Na_xWO_3. Alex agreed with these ideas and not only encouraged me but also invited me to give a talk in the IBM lab some months later. This was not bad for an early PhD student who had previously done rather little to sharpen his argument and did not have any real data at that time. Thus, I was obliged to grow

crystals, measure the electrochromic effects, solve a crystal structure and measure near-infrared absorption to confirm the existence of polaronic states in WO_3 and its doped analogues [3,4]. It took three years to establish a small laboratory for the investigation of perovskite structures in my home university in Hannover in Germany, with results coming out after 1975 [5,6]. When I returned to see Alex, he introduced me to Otwin Schirmer who was an expert in ESR spectroscopy. I worked with him for some years when he moved to Freiburg to the Frauenhofer Institut. We firmly established that the charge carriers in WO_3 are polarons [7,8]. Through Alex I met Harry Thomas in Basel with whom I worked on the quantum version of the Landau potentials [9], which proved useful to derive the low-temperature saturation effects and, ultimately, quantum fluctuations in $SrTiO_3$ [10]. I then spent time in the IBM lab and observed how Alex created an outstanding, international laboratory, which combined a great number of excellent people from different backgrounds. His leadership was very firm and helped me to a good start in science (and several visits to the 'Zunfthäuser an der Limmat'). In 2020, Alex returned to the investigation of superconductivity in reduced WO3 [11].

2. Results

While superconductivity in the WO_{3-x} materials is well established, the most intriguing property, which makes WO_3 unique, is its closeness to the metal-insulator transition which allows for an unusual phenomenon, as shown in Figure 1. The material undergoes a large number of phase transitions whereby almost all of them are ferroelastic. The transitions generate characteristic twin-domain networks [12–14]. These twin domains are separated by domain boundaries, which are simple twin walls along well-defined orientations. In WO_3, the domain boundaries persist in the ε phase at low temperatures [15]. When the sample is then cooled to ca. 3K, the domain walls—but not the rest of the sample—become superconducting [16,17].

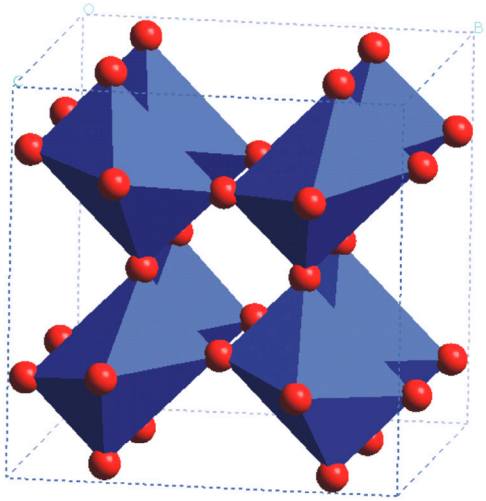

Figure 1. Structure of the tetragonal phase of the superconducting matrix.

The twin domain walls at higher temperatures are already highly conducting—much more so than the surrounding bulk [18]. Similar phenomena were subsequently found in many perovskite materials where the detailed conductivity mechanisms still remain obscure [19]. The effect in WO3 is much clearer by being based on the conduction by bipolarons (the recombination of two polarons into a bipolaron is shown in Figure 2). The domain boundary conductivity is more pronounced than in any other material discussed so far, as displayed in Figure 3.

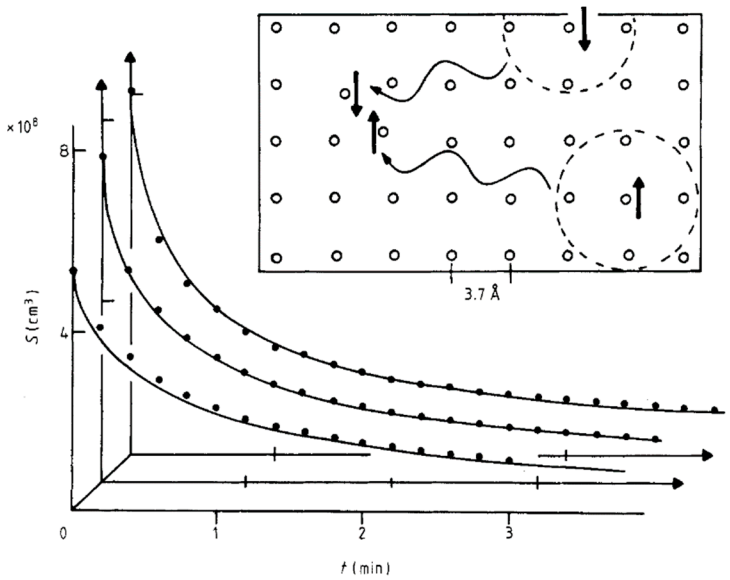

Figure 2. Sketch of the time dependence of the recombination of two polarons to form a bipolaron. Each polaron is marginally stable but does not represent the groundstate. The combination of two polarons form by spin pairing a bipolaron with lower energy. The bipolaron can be split by optical excitation. Once the bipolaron is split, it recombines over time (<60K).

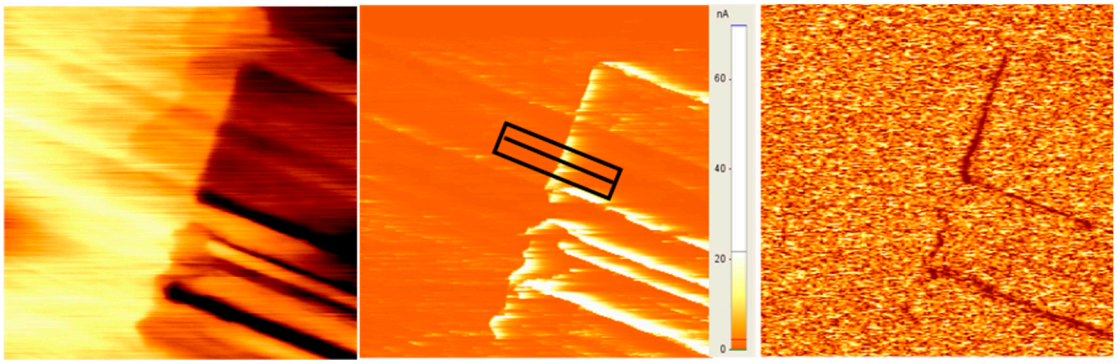

Figure 3. Topology (**left**), conductivity (**middle**) and piezoelectricity (**right**) of WO_3 at room temperature. This tetragonal phase is shown in Figure 1 and is piezoelectric. The piezoelectricity is short-circuited in the highly conducting domain walls, after [18].

First-principles investigations of bulk WO_3 [20] reproduce the essentials of the phase stability of the various crystallographic phases of WO_3. This work constituted a great step forward because it demonstrates that the initially observed deformation amplitudes during phase transitions are indeed related to specific properties of the interatomic bondings and the role of temperature in the form of larger lattice vibrations and increased entropy. It is revealed how a very simple binary compound possesses such a rich phase diagram and accordingly complex microstructures. Local polaronic deformations were calculated in a similar approach. The results are in excellent agreement with the free polaron electron density map of W^{5+} reported by Schirmer and Salje [7,8] from optical absorption and electron spin resonance (ESR) measurements. A single polaron has a 2D disk shape extended on a few neighbours. The possibility to stabilize this W^{5+} state allows us to characterize its electronic and structural properties through real space spin density, density of states analysis and the symmetry adapted mode analysis of the atomic distortion of the crystal. The first principle calculations by Bousquet et al [21] demonstrated how hard it is to capture polarons as physical objects of material science from first-principles calculations. This makes WO_3 a paradigmatic system to study polarons. Bousquet et al. [21] succeeded in calculating the energy and charge distribution of a single self-trapped polaron in WO_3 from density functional theory. Their calculations show that the

single polaron is at a slightly higher energy than the fully delocalized solution, in agreement with the experiments where a single polaron is an excited state of WO_3, as shown in Figure 4. The necessary stabilization energy stems from the spin–spin coupling and the common deformation cloud of the bipolaron. Bipolaron calculations in the first principle approach have still not been successful and are needed for a better understanding of the detailed electronic structure of a bipolaron.

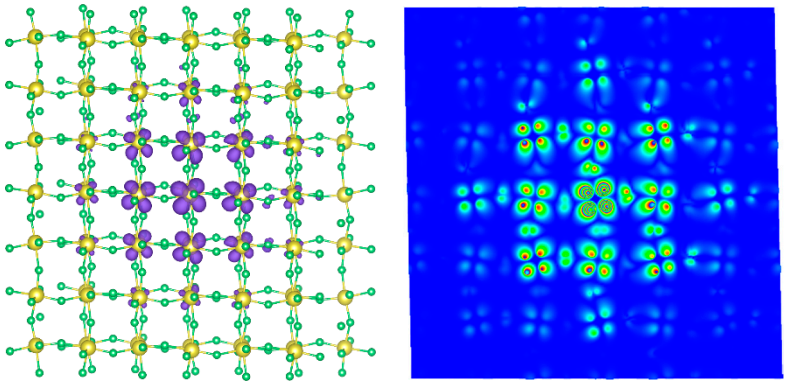

Figure 4. (**a**): 3D visualisation of the calculated density (B1WC functional) of the polaron in the xy plane of a WO_3 supercell (W and O atoms are in yellow and green respectively, the charge density is in purple); (**b**): 2D cut plane of the polaron density in the xy and xz planes passing through the central W atom where the charge localizes [21] Note the close similarity with the sketch in Figure 2.

The symmetry-adapted mode decomposition of the polaron distortions shows that, among numerous modes, a polar zone centre mode has the largest contribution and can be at the origin of the observed weak ferroelectricity of WO_3.

To analyse the electronic structure of the calculated polaron in WO_3, Figure 4 shows the total density of states (DOS) of a supercell with a self-trapped polaron [21]. The localized state appears in the gap of WO_3 in the spin up channel. This state in the gap corresponds to the d_{xy} state of W that slightly splits from the conduction bands (by about 0.4 eV), and it spreads over 0.1 eV in the gap. Hence, it is not fully localized, i.e., in agreement with what we observe from the real space density where the electron density of the polaron is spread over a few W atoms. This means that calculations simulate indeed a self-trapped single polaron in the $P2_1/c$ ground state phase of WO_3.

Interestingly, Reich and Tsabba [22] reported superconductivity, possibly related to the sample surface, at much higher temperatures (ca. 80K). Unfortunately, these observations could not be reproduced and remained uncertain and largely ignored. Recently, Muller and collaborators did indeed obtain some similar results. They reported that in samples with the composition $WO_{2.9}$, the signatures of superconductivity with the same transition temperature T_c = 80 K were registered by means of magnetization measurements. By lithium intercalation, the T_c was further increased to 94 K. The observed small superconducting fraction and the absence of clear transition in resistivity measurements indicate that the superconductivity is localized in small regions. No current percolation was found. In contrast, the earlier observation of W^{5+} - W^{5+} electron bipolarons in reduced tungsten oxide samples was confirmed [23].

They proposed that bipolarons form and cluster within crystallographic shear planes which exist in the Magneli phase of $WO_{2.9}$ ($W_{20}O_{58}$) and represent charge-carrier rich quasi-1D stripes or puddles [24]. The Magneli structural complexes are common not only in $W_{20}O_{58}$ but are locally present in pentagonal tungstate structures [24–26] and many other structures. It can hence be assumed that a much wider class of materials with W-O corner-sharing clusters exist, which may show similar puddle effects. This discovery clearly warrants substantially enhanced research to identify WO_3-derivatives where the coupling between the Magneli complexes in crystallographic shear planes (CS) percolate.

While there is no simple way to assess any superconductivity transition in these compounds, an early attempt where the necessary condition was formulated to obtain metallic conductivity in the normal state [23]. Polaronic systems often show metal–insulator (M–I) transitions as a function of the carrier concentration [27,28]. The M–I transition occurs near the 'overcrowding' point where the packing of polarons with diameters of around 0.5 nm reaches saturation. Geometrically, additional carriers cannot be condensed into polaronic states because the necessary lattice deformation is exhausted and carriers need to transfer to the conduction band. This 'overcrowding' point is possibly the critical point for the formation of carrier into puddles and filaments, which, in turn, promote local superconductivity.

3. Outlook

Superconductivity related to domain boundaries, CS planes, or other structural singularities are not just a simple addition to existing bulk properties, but represent a cornerstone of the emerging field of domain boundary engineering [29] where the domain boundary is the device and the bulk is simply the matrix to hold the domain boundary in space [30]. Novel device designs become possible. An example is a Josephson junction detector where the junction elements are the intersections of superconducting domain boundaries. As such domain boundaries can be designed to appear in high densities [31,32], such devices would have unsurpassed sensitivities and extremely small sizes. Similar effects appear in systems where mesoscopic inhomogeneities on the metal–superconductor transition occur in two-dimensional electron systems, typically at the interface between two perovskite materials. A model with mesoscopic inhomogeneities was considered [33] as a random-resistor network in effective medium theory. Particularly space correlations between the mesoscopic domains were found to dominate over random fluctuations. A typical example is then to utilise the two-dimensional electron gas at the $LaTiO_3/SrTiO_3$ or $LaAlO_3/SrTiO_3$ oxide interfaces, which becomes superconducting when the carrier density is tuned by gating. The measured resistance and superfluid density reveal inhomogeneous superconductivity related to the percolation of filamentary structures of superconducting "puddles" with randomly distributed critical temperatures, embedded in a nonsuperconducting matrix. This scenario is similar to the Magneli phases while the twin walls in WO_3 are, by definition, percolating over the distance of the length of the twin boundaries (which are often spanning from surface to surface). Previously, interfacial superconductivity was modelled using intrapuddle conductivity by a multiband system within a weak coupling BCS scheme [34]. The microscopic parameters, extracted by fitting the transport data with a percolative model, yield a consistent description of the dependence of the average intrapuddle critical temperature and superfluid density on the carrier density [35]. Clearly many of these interfacial features are similar in WO_3 twin boundaries and in $LaAlO_3/SrTiO_3$ oxide interfaces so that one can expect significant progress in either field from the comparison with the other [36,37].

Acknowledgment: EKHS is indebted to EPSRC for support (grant EP/P024904/1).
Conflicts of Interest: The author declares no conflict of interest.

References

1. Axe, J.D.; Shirane, G.; Mueller, K.A. Zone-boundary phonon instability in cubic $LaAlO_3$. *Bull. Am. Phys. Soc.* **1969**, *183*, 820.
2. Mueller, K.A.; Burkhard, H. $SrTiO_3$ Intrinsic quantum paraelectric below 4K. *Phys. Rev. B* **1979**, *19*, 3593–3602.
3. Salje, E. Non-stoichiometric tungsten compound, synthesis and lattice constants of WO_3-$NaWO_3$ mixed crystal compounds. *Z. Fur Allg. Angew. Chem.* **1973**, *396*, 267–270.
4. Salje, E. New type of electrooptic effect in semiconducting WO_3. *J. Appl. Crystallogr.* **1974**, *7*, 615–617.
5. Salje, E. Viswanathan K, Physical properties and phase transitions in WO_3. *Acta Crystallogr. Sect. A* **1975**, *31*, 356–359.
6. Salje, E. Lattice dynamics of WO_3. *Acta Crystallogr. Sect. A* **1975**, *31*, 360–363.

7. Schirmer, O.F.; Salje, E. Conducting bi-polarons in low-temperature crystalline WO_{3-x}. *J. Phys. C* **1980**, *13*, 1067–1072.
8. Schirmer, O.F.; Salje, E. W^{5+} polaron in low temperature crystalline WO_3 Electron spin resosnce and optical absorption. *Solid State Commun.* **1980**, *33*, 333–336.
9. Salje, E.K.H.; Wruck, B.; Thomas, H. Order parameter saturation and low temperature extension of Landau theory. *Z. Phys. Condens. Matter* **1991**, *82*, 399–404.
10. Kustov, S.; Luibimova, I.; Salje, E.K.H. Domain dynamics in quantum-paraelectric $SrTiO_3$. *Phys. Rev. Lett.* **2020**, *124*, 016801.
11. Shengelaya, A.; Conder, K.; Mueller, K.A. Signatures of filamentary superconductivity up to 94K in tungsten oxide $WO_{2.9}$. *J. Supercond. Nov. Magn.* **2020**, *33*, 301–306.
12. Locherer, K.R.; Swainson, I.P.; Salje, E.K.H. Phase trasitions in WO_3 at high temperatures—A new look. *J. Phys. Condens. Matter* **2002**, *11*, 6737–6756.
13. Howard, C.J.; Luca, V.; Knight, K.S. High-temperature phase transitions in tungsten trioxide—The last word? *J. Phys. Condens. Matter* **2002**, *14*, 377–387.
14. Viehland, D.D.; Salje, E.K.H. Domain boundary dominated systems, adaptive structures and functional twin boundaries. *Adv. Phys.* **2014**, *63*, 267–326.
15. Salje, E.K.H.; Rehmann, S.; Pobell, F.; Morris, D.; Knight, K.S.; Herrmannsdorfer, T.; Dove, M.T. Crystal structure and paramagnetic behaviour of epsilon-WO_{3-x}. *J. Phys. Condens. Matter* **1997**, *9*, 6563–6577.
16. Aird, A.; Salje, E.K.H. Sheet superconductivity in twin walls: Experimental evidence of WO_{3-x}. *J. Phys. Condens. Matter* **1998**, *10*, L377–L380.
17. Aird, A.; Domeneghetti, M.C.; Mazzi, F.; Salje, E.K.H. Sheet superconductivity in WO_{3-x}: Crystal structure of the tetragonal Matrix. *J. Phys. Condens. Matter* **1998**, *33*, L569–L574.
18. Kim, Y.; Alaxei, M.; Salje, E.K.H. Nanoscale properties of twin walls and surface layers in piezoelectric WO_{3-x}. *Appl. Phys. Lett.* **2010**, *96*, 032904.
19. Seidel, J.; Maksymovych, P.; Batra, Y.; Katan, A.; Yang, S.-Y.; He, Q.; Baddorf, A.P.; Kalinin, S.V.; Yang, C.-H.; Yang, J.-C.; et al. Domain wall conductivity in La doped $BiFeO_3$. *Phys. Rev. Lett.* **2010**, *105*, 197603.
20. Hamdi, H.; Salje, E.K.H.; Ghosez, P.; Bousquet, P. First-principles investigation of bulk WO_3. *Phys. Rev. B* **2016**, *94*, 245124.
21. Bousquet, E.; Hamdi, H.; Aguado-Puente, P.; Salje, E.K.H.; Artacho, E.; Ghosez, P. First-principles characterization of single-electron polaron in WO_3. *Phys. Rev. Res.* **2020**, *2*, 012052.
22. Reich, S.; Tsabba, Y. Possible nucleation of a 2D superconducting phase on WO3 single crystals surface doped with Na^+. *Eur. Phys. J. B* **1999**, *1*, 1–4.
23. Salje, E.K.H. Polarons and bi-polarons in WO_{3-x}. *Eur. J. Solid State Inorg. Chem.* **1994**, *31*, 805–821.
24. Shengekava, A.; Conder,K.; Mueller,K.A. Signatures of filamentary Superconductivity up to 94K in tungsten oxide WO2.90. *Journal of Superconductivity and Novel Magnetism* **2020**, 33, 301-306.
25. Viswanathan, K.; Salje, E. Crystal-structure and charge carrier behavior of (W12.64Mo1.36)O41 and its significance to other related compounds. *Acta Cryst.* **1981**, *37*, 4449–4456.
26. Viswanathan, K.; KBrandt, K.; Salje, E. Crysatl-structure and charge carrier concentration of $W_{18}O_{49}$. *J. Solid State Chem.* **1981**, *36*, 45–51.
27. Ruscher, C.; Salje, E.; Hussain, A. The effect of Nb-W distribution of polaronic transport in ternary Nb-W oxides- electrical and optical properties. *J. Phys. C-Solid State* **1988**, *21*, 4465–4480.
28. Ruscher, C.; Salje, E.; Hussain, A. The effect of polaron concentration on the polaron transport in $NbO_{2.5-x}$ Optical and electric properties. *J. Phys. C-Solid State* **1988**, *21*, 3737–3749.
29. Salje, E.K.H. Domain boundaries as active memory devices: Trajectories towards domain boundary engineering. *ChemPhysChem* **2010**, *11*, 940–950.
30. Catalan, G.; Seidel, J.; Ramesh, R.; Scott, J.F. Domain wall nanoelectronics. *Rev. Mod. Phys.* **2012**, *84*, 119–156.
31. Salje, E.K.H.; Ding, X.; Aktas, O. Domain glass. *Phys. Status Solidi B* **2014**, *251*, 2061–2066.
32. Ding, X.; Zhao, Z.; Lookman, T.; Saxena, A.; Salje, E.K.H. High junction and twin boundary densities in driven dynamical systems. *Adv. Mater.* **2012**, *24*, 5385–5389.
33. Caprara, S.; Grilli, M.; Benfatto, L.; Castellani, C. Effective medium theory for superconducting layers: A systematic analysis including space correlation effects. *Phys. Rev. B* **2011**, *84*, 014514.

34. Caprara, S.; Biscaras, J.; Bergeal, N.; Bucheki, D.; Hurand, S.; Feuillet-Palma, C.; Rastogi, A.; Budhani, R.C.; Lesueur, J.; Grilli, M. Multiband superconductivity and nanoscale inhomogeneity at oxide interfaces. *Phys. Rev. B* **2013**, *88*, 020504.
35. Scopigno, N.; Bucheli, D.; Caprara, S.; Biscaras, J.; Bergeal, N.; Lesueur, J.; Grilli, M. Phase separation from electron confinement at oxide interfaces. *Phys. Rev. Lett.* **2016**, *116*, 026804.
36. Dezi, G.; Scopigno, N.; Caprara, S.; Grilli, M. Negative electronic compressibility and nanoscale inhomogeneity in ionic-liquid gated two-dimensional superconductors. *Phys. Rev. B* **2018**, *98*, 214507.
37. Bovenzi, N.; Caprara, S.; Grilli, M.; Raimondi, R.; Scopigno, N.; Seibold, G. Density inhomogeneities and Rashba spin-orbit coupling interplay inoxide interfaces. *J. Phys. Chem. Solids* **2019**, *128*, 118–129.